Effect of structural modulation and thickness of a graphene overlayer on the binding energy of the Rashba-type surface state of Ir(111)

2013 New J. Phys. 15 115009

(http://iopscience.iop.org/1367-2630/15/11/115009)

New Journal of Physics
The open access journal for physics

Effect of structural modulation and thickness of a graphene overlayer on the binding energy of the Rashba-type surface state of Ir(111)

J Sánchez-Barriga[1,3], G Bihlmayer[2], D Wortmann[2], D Marchenko[1], O Rader[1] and A Varykhalov[1]

[1] Helmholtz-Zentrum Berlin für Materialien und Energie, Elektronenspeicherring BESSY II, Albert-Einstein-Strasse 15, 12489 Berlin, Germany

[2] Peter Grünberg Institut and Institute for Advanced Simulation, Forschungszentrum Jülich and JARA, 52425 Jülich, Germany

E-mail: jaime.sanchez-barriga@helmholtz-berlin.de

New Journal of Physics **15** (2013) 115009 (18pp)
Received 1 June 2013
Published 15 November 2013
Online at http://www.njp.org/
doi:10.1088/1367-2630/15/11/115009

Abstract. The Ir(111) surface is known to host a surface state with a giant spin–orbit splitting due to the Rashba effect. This surface state is stable even in air when Ir is protected with an epitaxial graphene overlayer. In the present paper, we reveal an effect allowing one to tune the binding energy of this spin-split surface state up and down and demonstrate the practical application of this effect by two different approaches. The first approach is related to a decoration of the moiré pattern of single-layer graphene on Ir(111) by self-assembled nanoclusters of different compositions. The clusters locally pin graphene to the Ir substrate and enhance the amplitude of its structural corrugation, which, in turn, leads to an *increase* in the surface state binding energy. The second approach is related to the synthesis of few-layer graphene on Ir(111) by segregation of carbon. Additional graphene layers induce a shift of the Ir surface state towards *lower* binding energies and bring it almost to the Fermi level. Based on density functional calculations performed for the graphene/Ir(111) system, we show that in both cases the effect causing the binding energy shifts is intimately related to the

[3] Author to whom any correspondence should be addressed.

distance between graphene and the Ir surface, which is subject to change due to deposition of clusters or by increasing the amount of graphene overlayers. In contrast, the observed spin–orbit splitting of the Ir(111) surface state remains remarkably robust and constant in all cases. Our theoretical analysis reveals that such stability can be explained by the localization properties of the Ir surface state that is a deep surface resonance.

Contents

1. Introduction

The Rashba effect is important for the creation of spin-polarized electronic states without any implication of ferromagnetism. It is based on the spin–orbit interaction and inversion symmetry breaking [1] and typically occurs at crystal surfaces and interfaces. The Rashba effect lifts the spin degeneracy of electronic states and results in a splitting of the electronic bands into subbands with opposite spin directions. These subbands are symmetrically displaced in momentum space and can be described by

$$E_{\pm}(\mathbf{k}_{\parallel}) = \frac{\hbar^2 \mathbf{k}_{\parallel}^2}{2m^*} \pm \alpha_{\mathrm{R}} |\mathbf{k}_{\parallel}|, \tag{1}$$

where m^* denotes the electron effective mass and α_{R} is the Rashba parameter of spin–orbit coupling. Both determine the magnitude of the momentum splitting of the spin subbands $\Delta\mathbf{k}_{\parallel}$ relative to the origin ($\mathbf{k}_{\parallel} = 0$) through the expression

$$\Delta\mathbf{k}_{\parallel} = \frac{m^* \alpha_{\mathrm{R}}}{\hbar^2}. \tag{2}$$

Tight-binding models and first-principles calculations for metal surfaces have shown that α_{R} depends on the intraatomic electric field along the direction perpendicular to the surface as well as on the asymmetry of the electronic wave functions near the nuclei of the surface atoms and their atomic number [2–4]. This means that the Rashba splitting is characteristic of surfaces and interfaces of high-Z materials and must be sensitive to the nuclear charge Z of the atomic constituents. This prediction has also been confirmed by experiments [5–9]. In the context

of transport properties, the Rashba effect is crucially important for spintronics since it may create dissipationless spin currents without the application of magnetic fields [10, 11]. To date, the largest Rashba splittings were achieved for interface states emerging in monolayers (ML) of H [12], Li [5], Au or Ag on W(110) [6], quantum-well states on W(110) [8], atomic Au chains [13], surface alloys of Bi with Ag(111) [14] and bulk BiTeI [9]. Recently, we have found that Ir(111) also hosts a surface state with a giant Rashba-type spin–orbit splitting characterized by $\alpha_R \sim 3.05 \times 10^{-10}$ eV m [7]. This system is particularly interesting, as we have shown that in addition the surface state can be protected from the environment by growing an epitaxial graphene layer on top of the Ir crystal. The protection is so reliable that the surface state persists even when the sample is taken in an ambient atmosphere [7]. Such protected spin-polarized states can be of great importance for applications in spintronics.

In the present work, we explore further intriguing properties of the graphene/Ir(111) system and show that graphene can be used to enable a modification of the electronic structure of the Ir(111) surface state. In particular, we show that the binding energy of the Ir surface state varies with the interfacial separation between graphene and Ir, while the spin–orbit splitting of the Ir surface state remains preserved. We demonstrate how this effect can be exploited practically in the framework of two different approaches. The first approach involves nanopatterning of single-layer graphene on Ir(111) with periodic arrays of small clusters of different compositions. It is known that ∼10% lattice mismatch between graphene and Ir leads to the occurrence of a pronounced moiré pattern in graphene with a lateral periodicity of ∼25 Å [15–18]. It is also established that such a periodic pattern can be decorated by self-assembled nanoclusters [19–21]. Here we show that due to its protection by the graphene the Ir(111) surface state survives the deposition of Ir, Au and Fe clusters, and that the presence of the clusters leads to an increase of the binding energy of the Ir surface state by about 90–100 meV. Our earlier studies suggest that the binding energy of the Ir surface state depends on the proximity to the graphene adlayer [7]. Connected to this, we show that the observed behaviour of the surface state can be attributed to a local pinning of the graphene by the clusters. The pinning enhances the structural corrugation and with it the amplitude of the moiré modulation [22], which, in turn, increases the average distance between graphene and the Ir(111) substrate.

The second approach leading to a modification of the surface state binding energy does not involve nanopatterning but thickness control of the epitaxial graphene overlayer. We have achieved accurate layer-by-layer growth of graphene on Ir(111) and have found that the effect of graphene thickness on the Ir surface state is opposite to the effect of deposited clusters. Here we show that formation of each additional graphene layer leads to an overall shift of the Ir(111) surface state towards lower binding energy. In particular, the binding energy of the Ir surface state changes from its original value of ∼ 340 to ∼ 95 meV, and then back to ∼150 meV upon formation of two and three graphene layers, respectively. Similarly to the case of nanoclusters, we show that the origin of the observed evolution of the surface state binding energy can be ascribed to the distance between the Ir(111) substrate and the first graphene layer, which decreases upon formation of additional layers due to their interaction with the substrate through van der Waals forces. We also show that the magnitude of the spin–orbit splitting of the Ir surface state under graphene changes neither for deposited clusters nor for few-layer graphene grown on top of the Ir substrate.

Because of the apparently strong relation of the observed effects to the distance between Ir(111) and the graphene overlayer, we have investigated the evolution of the surface state binding energy with the graphene–Ir(111) distance by means of density functional theory

(DFT) calculations. Our theoretical analysis provides good correlation with the experimental observations and confirms our interpretation involving a structural relaxation of the graphene adlayers. Our calculations of the localization properties of the Ir(111) surface state also reveal and explain its robustness against adsorption of graphene and deposition of self-assembled nanoclusters.

2. Methods

Angle-resolved photoemission (ARPES) measurements were performed with the ARPES 1^2 endstation at the UE112-PGM2a beamline of BESSY II. Spin-resolved experiments (spin-ARPES) were conducted at the UE125/2-SGM beamline with the recently developed RGBL-2 setup equipped with a combination of a two-dimensional micro-channel plate and a Mott-type spin detector, allowing us to simultaneously acquire both the in-plane and out-of-plane components of spin. In all cases a photon energy of $h\nu = 62$ eV and linear (s+p) polarization of light were employed. Photoemission spectra were acquired either at room temperature or at a temperature of $T = 40$ K. STM characterization was done at room temperature in a separate vacuum chamber equipped with an Omicron VT scanning tunneling microscope (STM) using polycrystalline W tips carefully prepared as described elsewhere [23].

The clean Ir(111) substrate was prepared by repeated cycles of ion sputtering (Ar^+, 2500 eV) and annealing at 1500 K. The single layer of epitaxial graphene on Ir(111) was synthesized by chemical vapour deposition (CVD) of propylene at a partial pressure of 3×10^{-8} mbar and a sample temperature of $T = 1100$ K. Additional graphene layers were prepared by segregation of carbon from the Ir bulk [24] with the assistance of subsurface hydrogen impregnated on the Ir crystal. Consistently with the literature [25], we have found that hydrogen significantly improves the quality of additionally segregated graphene layers and allows us to fabricate uniform few-layer graphene films of mm-large dimensions and homogeneous thickness.

It is known that graphene on Ir(111) may exhibit various rotational displacements [17, 26, 27]. This occurrence can be controlled by tuning the sample temperature and the partial pressure of hydrocarbons during the CVD procedure. All results presented in this work refer to the conventional rotational variant of graphene (the so-called $R0^\circ$ phase), which is aligned with Ir(111).

Superlattices of clusters were fabricated by deposition of Ir, Au or Fe atoms on single-layer graphene on Ir(111) from sources heated by electron bombardment and at low deposition rates of ~ 0.01 ML min^{-1}. In agreement with the literature [19], we have found that arrays of Ir clusters can be fabricated on moiré-patterned graphene by deposition at room temperature, while the growth of Au clusters required low-temperature deposition ($T = 40$ K). The growth of Fe clusters, which is reported here for the first time, also required low-temperature deposition.

Our theoretical results were obtained by DFT calculations in the generalized gradient approximation using the FLEUR code (see http://www.flapw.de for a program description). The code implements the full-potential linearized augmented plane wave method [28] and the Green function embedding method [29] and thereby allows the effective treatment of transition metal surfaces in a truly semi-infinite geometry. The Bloch spectral function for graphene on Ir(111) was calculated assuming an in-plane lattice constant of 2.71 Å and a surface region consisting of two Ir and one commensurate graphene overlayer embedded on the semi-infinite Ir substrate.

3. Results

3.1. The Ir(111) surface state

We start with the results of our characterization of the Rashba-split Ir(111) surface state, which is the central subject of our study. The physical properties of this surface state have already been addressed in detail in our earlier work [7]; therefore, here we will review these properties only briefly. The Ir(111) surface state evolves at the $\overline{\Gamma}$ point of the Ir(111) surface Brillouin zone (SBZ) within a surface-projected spin–orbit band gap of bulk Ir. According to our photon energy dependent studies, the surface state branches off the Λ_6^1 and Λ_6^3 bulk Ir bands [7] and reveals a downward dispersion with negative effective mass. The Ir surface state exhibits a giant spin splitting with $\alpha_R \sim 3.05 \times 10^{-10}$ eV m that corresponds to a momentum splitting of $\Delta\mathbf{k}_\parallel = 0.04$ Å^{-1}. For bare Ir(111) the surface state occurs at a binding energy of 340 meV (upper edge of the spin subbands). Synthesis of a single graphene layer on top of Ir(111) effectively protects the surface state but on the other hand shifts it towards lower binding energy to a value of about 190 meV due to interaction between graphene and Ir(111). Remarkably, the magnitude of the Rashba splitting is not affected by adsorption of graphene which establishes the high atomic number Z of Ir as the origin of the observed splitting [7].

The $E(\mathbf{k}_\parallel)$ dispersion of the Ir surface state sampled by ARPES from the Ir(111) surface covered with a single graphene layer is displayed in figure 1(a) and clearly shows a Rashba-type splitting of the band structure. The presence of the $R0^\circ$ rotational variant of graphene on top of Ir is evidenced by the low-energy electron diffraction (LEED) pattern shown in figure 1(b) and correspondingly by the STM image in figure 1(c), revealing a pronounced hexagonal moiré pattern due to lattice mismatch between graphene and the Ir substrate. As found by STM, the lateral periodicity of the moiré superstructure is ∼25 Å. Figure 1(d) reports several constant-energy surfaces (cuts 1–3) and the corresponding $E(\mathbf{k}_\parallel)$ dispersion (cut 4) extracted from the full photoemission mapping of the Ir surface state bands in figure 1(a). One can observe how the spin splitting evolves in two contours of circular shape corresponding to the subbands of opposite spin circulation. The spin character of the observed splitting can be directly confirmed by spin-ARPES. Figure 1(e) reports spin-resolved spectra of the surface state peak sampled at $k_\parallel = 0.15$ Å^{-1} and -0.1 Å^{-1} electron wave vectors and for spin components aligned in the plane of the Ir(111) surface. Very clearly, the in-plane spin-splitting reverses for electron wave vectors of opposite sign. The bottom panel of figure 1(e) displays the corresponding projections of the surface state spins on the axis perpendicular to the Ir(111) surface and reveals that the out-of-plane spin components are zero. These observations indicate that the surface state spins are rigidly aligned with the Ir surface plane and locked to the electron wave vector. Such behaviour is a hallmark of the Rashba effect and shows that the Ir surface state fully complies with the Rashba scenario. The band and spin structures of the Ir surface state are sketched in figure 1(g).

3.2. Effect of Ir and Au clusters on the binding energy of the Ir(111) surface state

Let us demonstrate how nanoclusters deposited on graphene/Ir(111) influence the electronic and spin properties of the Ir(111) surface state. We start with the case of Au and Ir clusters. These materials are non-magnetic but have a high atomic number resulting in a strong spin–orbit interaction in the electronic structure. We have already studied the effect of Ir and Au cluster superpotentials on the Dirac cone dispersion in graphene on Ir(111) and have shown that deposition of sub-monolayer amounts of Ir (Au) atoms is accompanied by their self-assembly

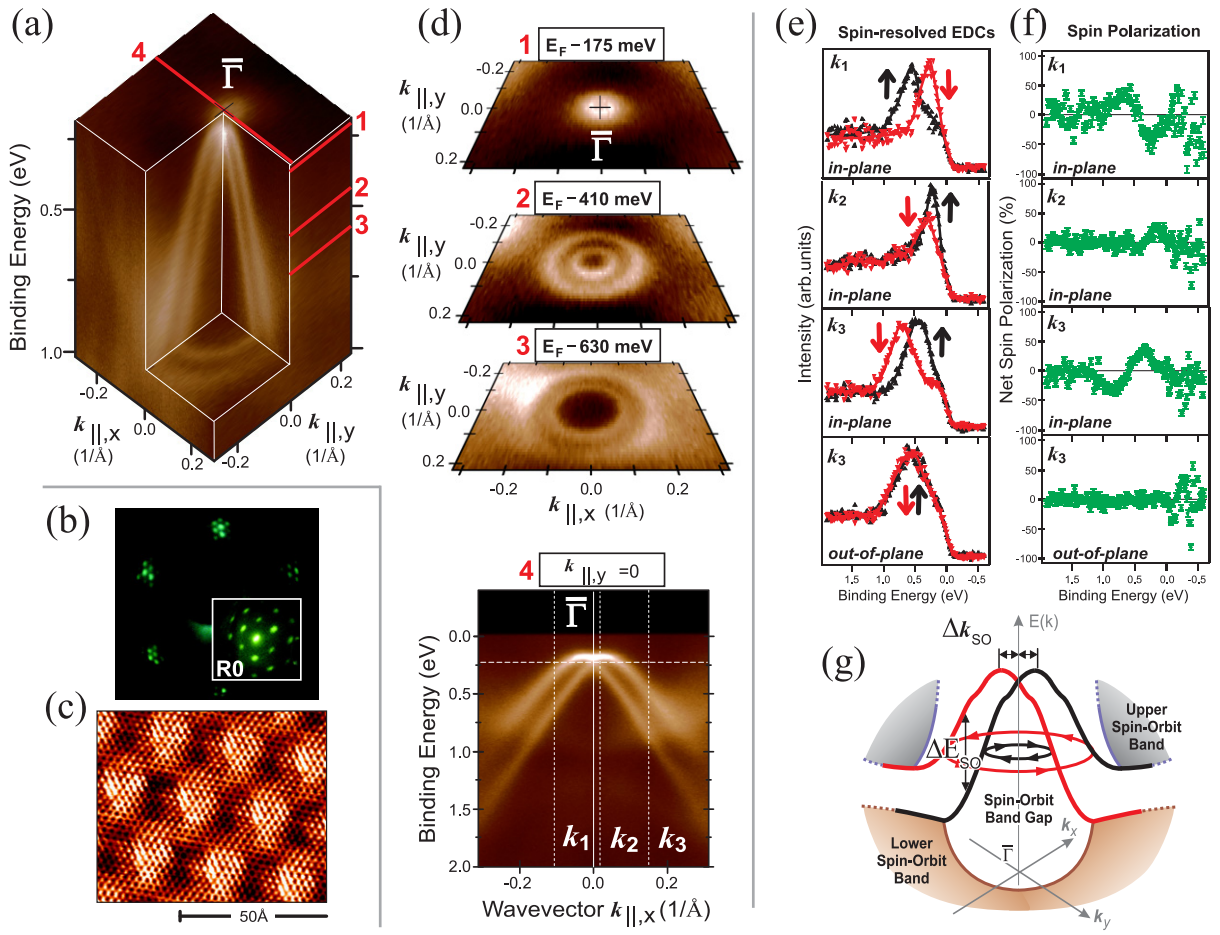

Figure 1. (a) The $E(\mathbf{k}_\parallel)$ dispersion of the Ir surface state sampled by ARPES from the Ir(111) surface covered with a single graphene layer clearly shows a Rashba-type splitting of the band structure. (b) The presence of the $R0^\circ$ rotational variant of graphene on top of Ir is evidenced by (b) the LEED pattern and correspondingly by (c) the STM image revealing a pronounced hexagonal moiré pattern due to lattice mismatch between graphene and the Ir substrate. (d) Several constant energy surfaces (cuts 1–3) and $E(\mathbf{k}_\parallel)$ dispersion (cut 4) extracted from the full photoemission mapping of the Ir surface state bands. (e) Spin-resolved spectra (energy distribution curves (EDCs)) of the surface state peak sampled at $k_\parallel = 0.15$ and $-0.1\,\text{Å}^{-1}$ electron wave vectors. Spin components aligned in the plane and out of the plane of the Ir(111) surface are shown. (f) Corresponding spin polarizations parallel and perpendicular to the Ir(111) surface. In agreement with the Rashba scenario, the in-plane spin projections reverse from negative to positive $k_\parallel$ electron wave vectors and the out-of-plane spin components are zero. (g) Sketch of the band and spin structures of the Ir surface state.

in highly periodic superlattices of nanoclusters due to decoration of the moiré pattern [21]. For every nominal concentration of Ir (Au) deposited on top of graphene/Ir(111), the adatoms equally distribute over moiré cells, culminating in the formation of very uniform clusters with dimensions proportional to the amount of deposited material. A superlattice of such clusters

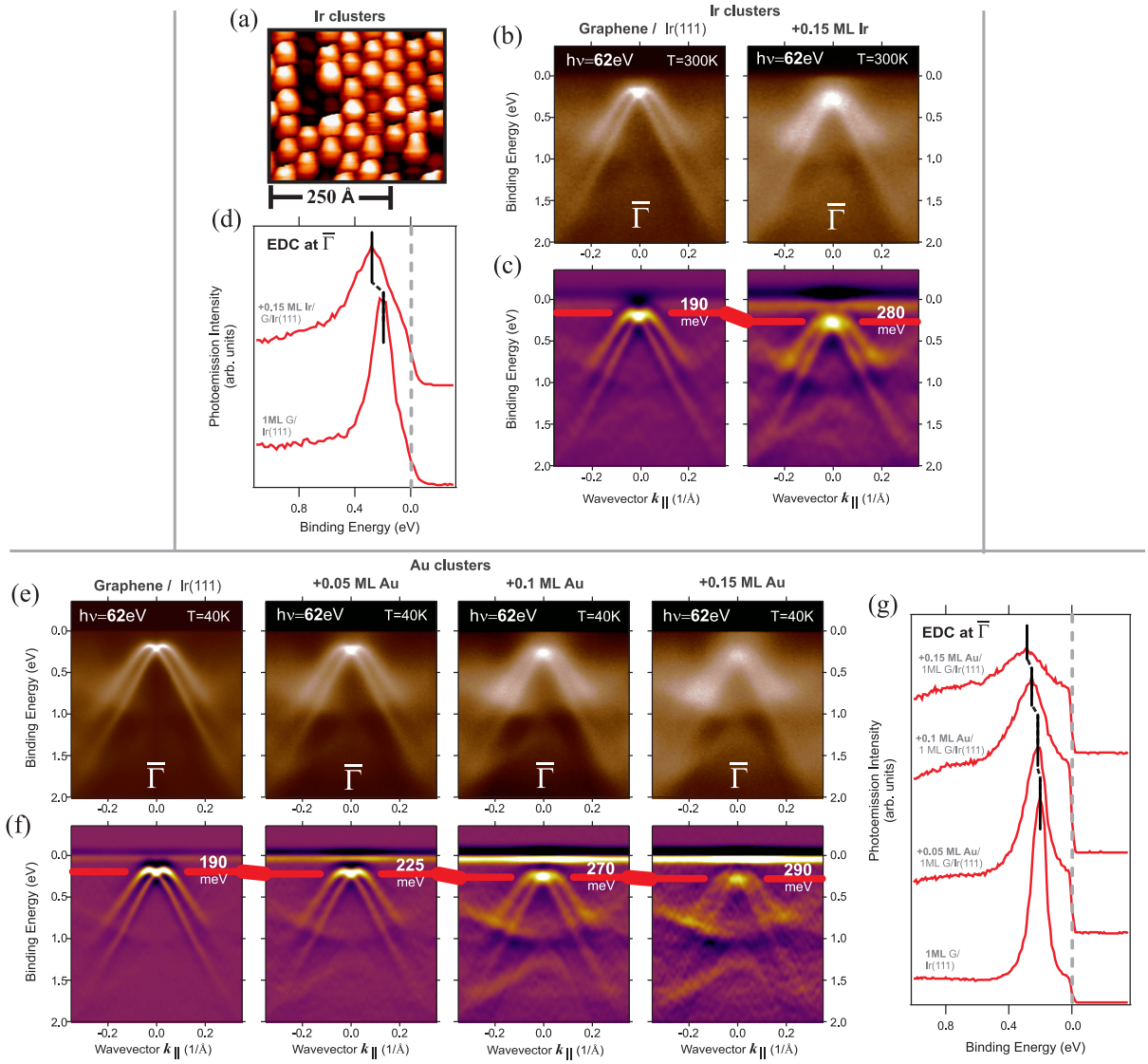

Figure 2. (a) Superlattice of clusters as observed by STM at room temperature after assembling from 0.15 ML of Ir on the graphene moiré. (b) Evolution of the Ir surface state under graphene with the growth of Ir clusters on top of the graphene moiré. The band structure of the surface state before and after the deposition of 0.15 ML Ir clusters is shown. (c) Second derivative $\frac{d^2I}{dE^2}$ of the ARPES data from figure 2(b). Evolution of the energetic position of the upper edge of spin subbands is marked with horizontal red lines. (d) Binding energy change of the surface state peak in EDCs sliced at the $\overline{\Gamma}$-point of the SBZ. (e) Modification of the Ir(111) surface state with the growth of Au clusters on top of the graphene moiré at $T = 40$ K. (f) Second derivatives of (e). (g) EDCs at the $\overline{\Gamma}$-point of (e).

assembled from 0.15 ML of Ir on the moiré of graphene is reported by STM in figure 2(a). The results shown are found to be in agreement with the literature [19]. The case of Ir adatoms is special and remarkable: arrays of Ir clusters are perfectly stable at room temperature for

any moderate Ir concentration. This simplifies the experiments significantly. In contrast, the persistence of periodic and ordered Au clusters requires a low temperature of the sample that has to be maintained throughout deposition and measurements.

Figure 2(b) presents the evolution of the Ir surface state under graphene with the growth of Ir clusters on top of the graphene moiré at room temperature. The band structure of the surface state under graphene is shown before and after the deposition of 0.15 ML of Ir atoms. One can see that the Ir surface state survives the deposition of high amounts of adatoms, even if its bands become broader when the clusters reach larger dimensions. In order to emphasize the dispersion of the broadened surface state, we display in figure 2(c) the second derivative $\frac{d^2I}{dE^2}$ of the ARPES data from figure 2(b). Besides the band broadening, a remarkable observation is the increase of the binding energy of the surface state with enlargement of clusters. The evolution of the energetic position of the upper edge of spin subbands is marked in figure 2(c) with horizontal lines. Alternation of the binding energy of the surface state peak is also clearly seen in the energy distribution curves (EDCs) sliced at the $\overline{\Gamma}$-point of the SBZ in figure 2(d). For 0.15 ML of deposited Ir the energy shift of the surface state amounts to ∼90 meV.

Figures 2(e) and (f) report a modification of the Ir(111) surface state with the growth of Au clusters on top of the graphene moiré at $T = 40$ K. The corresponding EDCs sliced at the $\overline{\Gamma}$-point of the SBZ are shown in figure 2(g). Good uniformity and high periodicity of the clusters were evidenced by the enlargement of *umklapp*-induced minigaps in the Dirac cone of graphene, which is the fingerprint of enhanced modulation of graphene by external superpotentials [20, 21]. It is clearly seen that the broadening of the photoemission peaks of the Ir surface state and its binding energy shift are very similar to the case of Ir clusters. The energy shift of the surface state amounts to ∼100 meV for ∼0.15 ML of deposited Au.

3.3. Effect of Fe clusters on the binding energy and Kramers degeneracy of the Ir(111) surface state

It would be interesting to study the effect of ferromagnetic clusters on the properties of the Ir(111) surface state under the graphene. Here, in principle, one may expect several phenomena related to the magnetic properties of the clusters. Firstly, their magnetic moments (if aligned along the surface plane) may interact with the spin–orbit split bands of the surface state and give rise to the so-called 'Rashba+Exchange' [30] effect, which causes energy shifts of the momentum-split spin subbands depending on the orientation of the cluster magnetization. Another possible effect would emerge if the magnetic moments of the clusters are directed perpendicular to the surface. In this case the distortion of the time-reversal symmetry can destroy the Kramers point, i.e. the crossing point of Rashba-split spin subbands, and open a band gap there [31].

We have deposited Fe on graphene/Ir(111) at a temperature of $T = 40$ K and examined the evolution of the Ir surface state. The results are reported in figure 3. First of all we have tested whether Fe indeed grows in clusters. Figure 3(a) shows the evolution of the graphene Dirac cone with the concentration of deposited Fe increasing up to 0.13 ML. One can clearly see that the Dirac cone moves towards higher binding energy and the band gap at the Dirac point (red arrow) and the *umklapp*-induced minigaps (blue lines) enlarge with increasing Fe cluster concentration. Such behaviour is characteristic of an enhanced potential of the superlattice modulation [20, 21] and is a fingerprint of cluster formation. The increased width of the minigaps is emphasized in figure 3(b) where EDCs are traced through the minigaps and shown

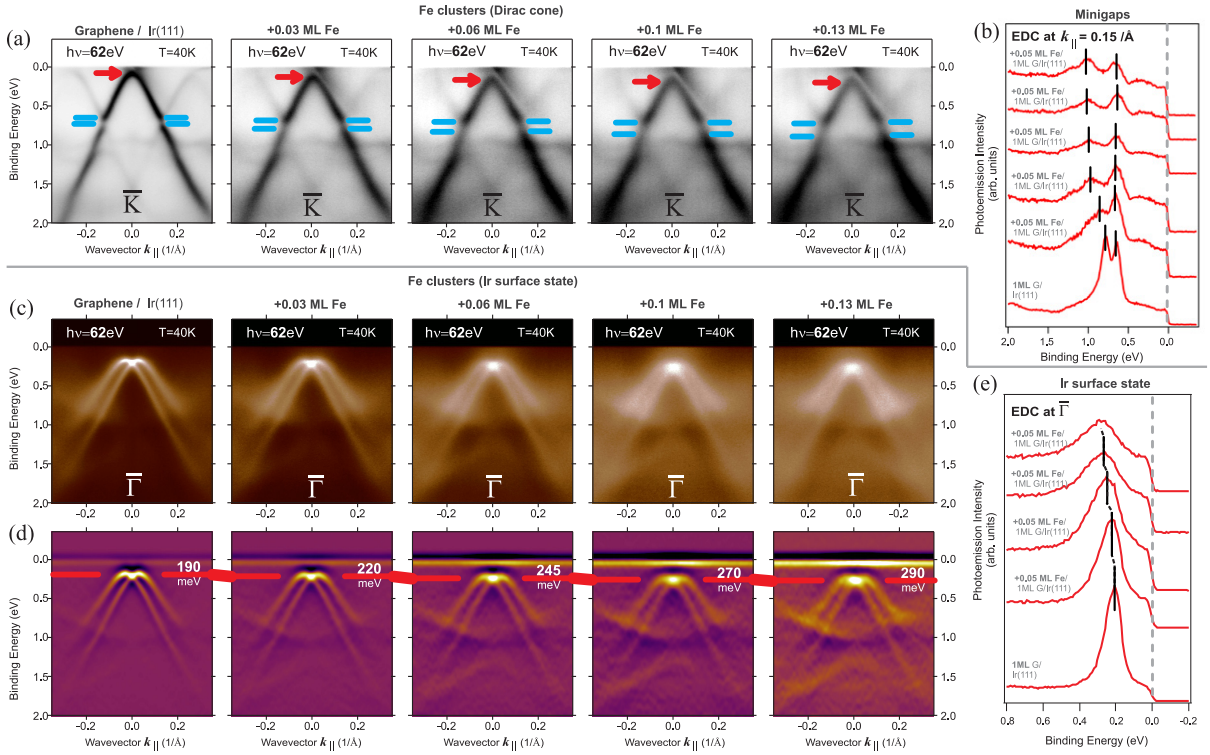

Figure 3. (a) Evolution of the graphene Dirac cone with deposited Fe increasing up to 0.13 ML. The Dirac cone moves towards higher binding energy. The band gap at the Dirac point (red arrow) and the *umklapp*-induced minigaps (blue lines) enlarge with increasing Fe cluster concentrations. (b) The increased width of the minigaps is emphasized by EDCs traced through the minigaps for different Fe concentrations. (c) Evolution of the Ir(111) surface state with enlargement of Fe clusters (increasing concentration of deposited Fe). (d) Second derivative $\frac{d^2I}{dE^2}$ of the ARPES data from (c). Evolution of the energy position of the upper edge of spin subbands is marked with horizontal lines. (e) EDCs at the $\overline{\Gamma}$-point of (d).

for different Fe concentrations. Careful analysis reveals that the energy shift of the Dirac cone as well as enlargement of the minigaps and the gap at the Dirac point are identical to the case of graphene/Ir(111) deposited with Ir and Au clusters of equivalent concentrations [21]. These findings show that modifications of the electronic structure of graphene due to cluster growth are of universal character and do not depend on the chemical character of the clusters.

Figures 3(c) and (d) show the evolution of the Ir(111) surface state with the enlargement of Fe clusters (increasing concentration of deposited Fe). The surface bands undergo a shift towards higher binding energy by about 100 meV (see also figure 3(e)) and the spin–orbit splitting remains preserved in the presence of Fe. This behaviour is identical to the case of graphene patterned with arrays of Ir and Au clusters. Obviously, neither a 'Rashba+Exchange' effect nor the destruction of the Kramers point are observed, which indicates that the Ir surface state is robust against the perturbations of graphene with disordered magnetic moments. We will return to this point in the discussion below.

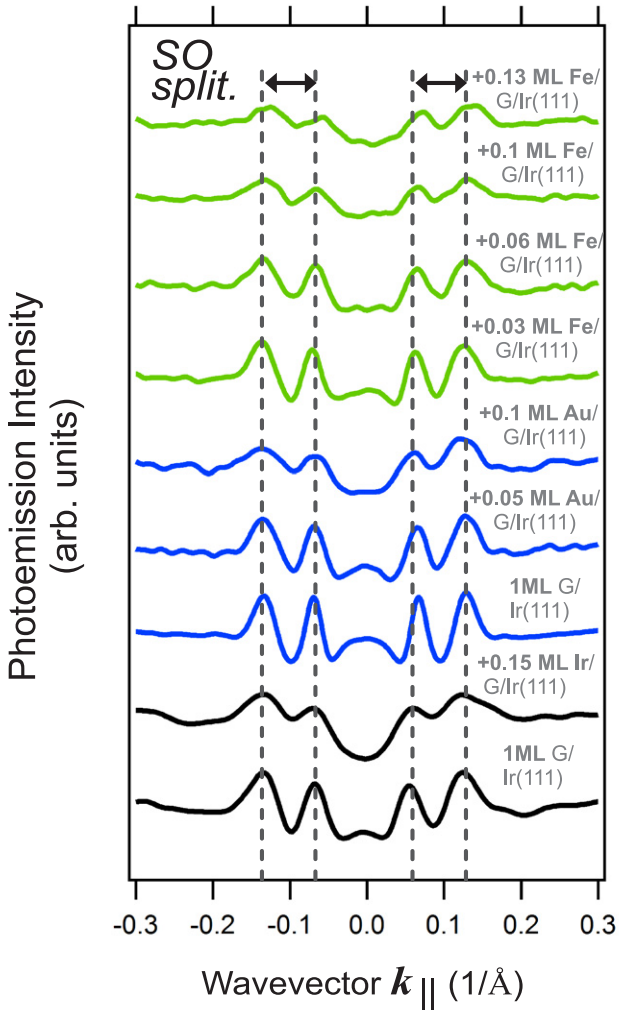

Figure 4. Set of momentum distribution curves (MDCs) of the Ir(111) surface state (profiles of the ARPES dispersions along the $\mathbf{k}_{\|}$ axis) traced at a relative binding energy of 0.3 eV with respect to the Kramers point for graphene patterned with Ir, Au and Fe clusters (black, blue and green MDCs, respectively). Analysis of the momentum splitting shows that the Rashba splitting of the surface state is not affected by the clusters. It appears sensitive neither to the nuclear charge of the cluster materials nor to the cluster size (strength of the lateral superpotential modulation).

3.4. Effect of clusters on the Rashba splitting of the Ir(111) surface state

We have taken particular care to test how the clusters affect the magnitude of Rashba splitting of the Ir(111) surface state. Although $_{26}$Fe is a light material and cannot create an extrinsic spin–orbit effect (exactly as $_{27}$Co and $_{28}$Ni [32, 33]) the situation with high-Z materials $_{79}$Au and $_{77}$Ir can be very different. We have earlier demonstrated that contact of graphene to a monolayer of Au or to Ir(111) results in a giant Rashba splitting of the graphene Dirac cone that can reach values up to about 100 meV [27, 34, 35]. Hence, it is possible that clusters of high spin–orbit materials decorating the graphene moiré can also influence the Rashba splitting of the Ir surface state under graphene. Figure 4 reports a set of momentum distribution curves (MDCs) of the

Ir(111) surface state (profiles of the ARPES dispersions along the $\mathbf{k}_{\|}$ axis) traced at equivalent binding energies (0.3 eV from the Kramers point) for graphene patterned with Ir, Au and Fe clusters of different dimensions. Careful analysis of the momentum splitting shows that the Rashba splitting of the surface state is not affected by the clusters. It appears sensitive neither to the nuclear charge of the cluster materials nor to the cluster size (strength of the lateral superpotential modulation).

3.5. Effect of few-layer graphene on the band structure of the Ir(111) surface state

We have shown above that the binding energy of the Ir(111) surface state can be increased by nanopatterning of a single graphene overlayer with clusters of different compositions. However, in the general context of applications it is required that spin-split bands cross the Fermi energy. Hence, it is more desirable to find a way to decrease the binding energy of the Ir surface state. We have established such an approach leading to a shift of the Rashba-split surface state into the vicinity of the Fermi level.

This approach is related to the formation of several graphene layers on top of Ir(111) by segregation of carbon from the Ir bulk. Figures 5(a) and (b) report the evolution of the Ir(111) surface state from the bare Ir surface to a surface covered with three graphene layers. One can see from the ARPES dispersions of the Ir surface state and the EDC profiles in figure 5(c) that the formation of two graphene layers decreases the binding energy of the Ir surface state while the formation of a third graphene layer reverses the process. It is seen that the surface state changes its binding energy from $\sim$340 meV (bare Ir(111)) to $\sim$ 95 meV (Ir(111) with a graphene bilayer) and then back to 150 meV (Ir(111) with a graphene trilayer). We emphasize that formation of high-quality bilayer and trilayer graphene is evidenced by characteristic double- and triple-split Dirac cones seen in the ARPES dispersions of figure 5(d). The diagram in figure 5(f) plots the binding energy of the upper edge of the surface state bands versus the amount of graphene layers. As seen from the diagram, the shift of the binding energy comes to saturation after two graphene layers are formed and then reverses. Moreover, the Rashba splitting of the surface state is not affected by few-layer graphene (see figure 5(e)).

It is remarkable that few-layer graphene not only moves the Ir(111) surface state towards the Fermi energy but also preserves the sharpness of the surface state bands. In contrast to the case of deposited clusters that act as defects and cause significant broadening of the surface state bands (figures 2 and 3), few-layer graphene does not induce any defects and keeps linewidths of the spin subbands intact.

4. Discussion

Let us discuss why the Ir(111) surface state binding energy depends on the strength of the cluster superpotential and on the thickness of the graphene overlayer. We start the analysis for the clusters. A rather rational explanation of the binding energy change could be a charge doping of graphene from the clusters which results in the creation of an electric dipole at the graphene–Ir interface. There are, however, several arguments against such an interpretation. The first argument is the nature of the Ir(111) surface state. We have performed DFT calculations and investigated the localization and orbital character of the surface state in the presence of graphene. Spatial maps of its charge density calculated at the centre of the Brillouin zone $\overline{\Gamma}$ ($k_{\|} = 0\,\text{Å}^{-1}$) and for $k_{\|} = 0.2\,\text{Å}^{-1}$ are shown in figures 6(a) and (b), respectively. One can see

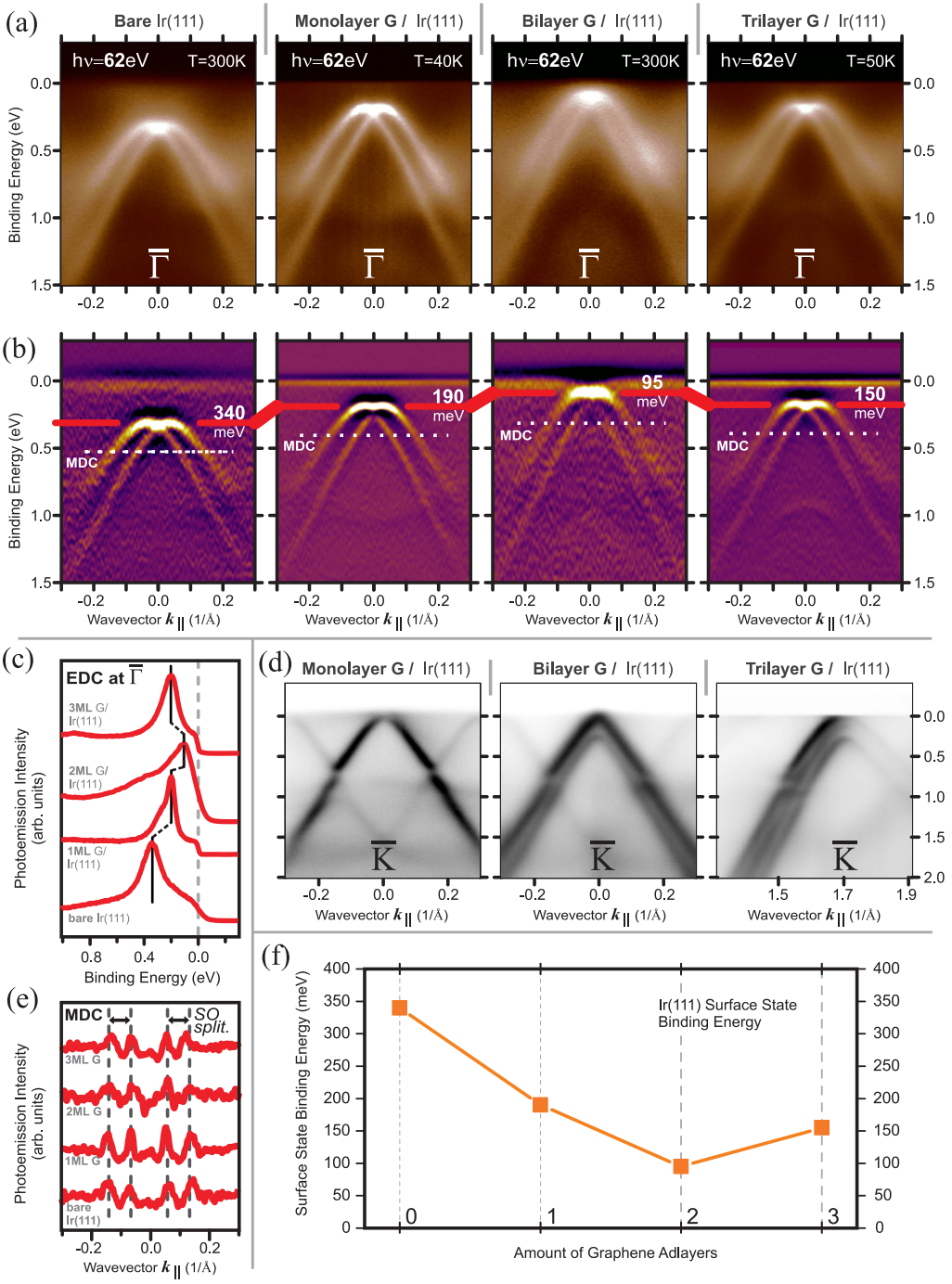

Figure 5. (a) Evolution of the Ir(111) surface state from the bare Ir surface to the surface covered with three graphene layers. (b) Second derivative $\frac{d^2I}{dE^2}$ of the ARPES data shown in (a). (c) EDC profiles at $\overline{\Gamma}$ extracted from (a). (d) Formation of high-quality bilayer and trilayer graphene is observed by characteristic double- and triple-split Dirac cones seen in ARPES dispersions. (e) Corresponding MDCs showing that the Rashba splitting of the surface state is not affected by few-layer graphene. (f) Dependence of the binding energy of the upper edge of the surface state bands on the number of graphene layers.

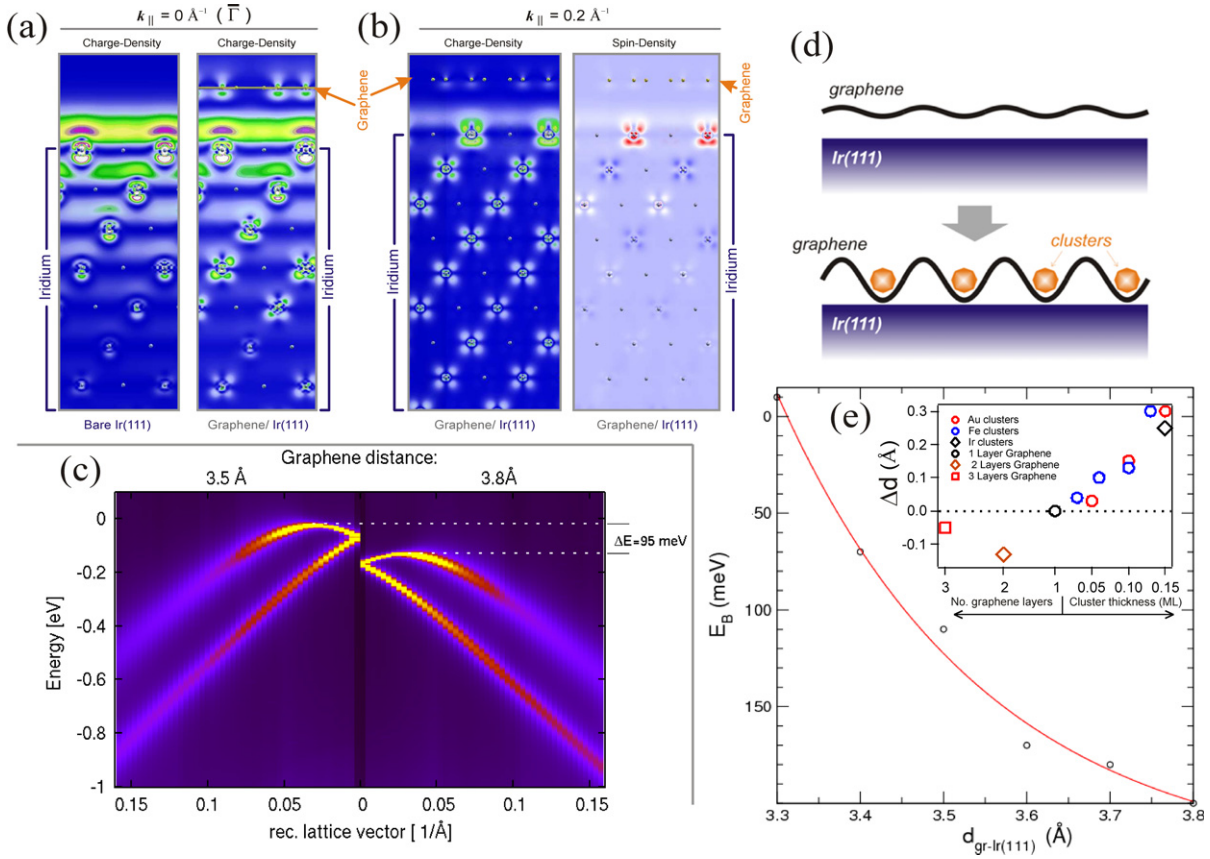

Figure 6. (a), (b) Spatial maps of surface state charge and spin density calculated at $\overline{\Gamma}$ ($k_\parallel = 0\,\text{Å}^{-1}$) and for $k_\parallel = 0.2\,\text{Å}^{-1}$. Only near the $\overline{\Gamma}$-point has the Ir surface state a free-electron-like p_z orbital character and rapidly decays into the Ir bulk. (c) Comparison of the band structure of the surface state calculated for two distances providing a binding energy difference of 95 meV (energy shift similar to the shifts observed in the experiments upon deposition of large clusters (0.15 ML)). (d) Sketch of the proposed mechanism of structural relaxation. (e) Calculated dependence of the Ir surface state binding energy on the distance to graphene. Inset: variation of the relative graphene–Ir distance (Δd) in the ARPES experiment. The values of Δd were extracted by comparing the relative shifts of the Ir surface state in the experiment to the theoretical calculations in (e).

that only near the $\overline{\Gamma}$-point has the Ir surface state a free-electron-like p_z orbital character and rapidly decays into the Ir bulk. For all wave vectors off $\overline{\Gamma}$, the surface state exhibits a pronounced $d_{x,z}$ character and propagates deeply into the bulk of the Ir crystal. As seen in figure 6(b), the states are spin-polarized and the polarization reverts between the topmost Ir layer and the layers underneath. This means that the Ir(111) is rather a deep surface resonance that should not be sensitive to weak electric dipoles induced by graphene doping. This is also in agreement with our findings that formation of one graphene layer on top of Ir(111) does not shift the Ir 4f core levels [7] but moves the surface state by about 150 meV towards lower binding energy (see figure 5(b)), indicating a relatively weak graphene–Ir interaction.

The second argument against charge doping is the independence of the Ir surface state behaviour from the cluster material, i.e. the chemical element. Indeed, the observed energy shift of the surface state with enhanced modulation by clusters is identical for Au, Ir and Fe clusters. This is quite unexpected within a doping scenario, since we know that contact of graphene with Ir and Au results in p-doping [20, 21, 35, 36], while contact with 3d-metals (Ni, Co and Fe) causes n-doping and an opposite energy shift of the π-band [34, 37, 38]. In addition, the doping of graphene by Ir clusters seen in C1s x-ray photoelectron spectra in [21] was found to be much less (<50 meV) than the cluster-induced energy shift of the Ir surface state ($\sim$90–100 meV).

Having excluded charge doping as the origin of the observed changes in the binding energy of the Ir(111) surface state, we propose a model based on structural relaxation of the graphene layer induced by deposited clusters. Indeed, by comparing ARPES dispersions shown in figure 5(a) for bare Ir(111) and for Ir(111) covered with one graphene layer, we anticipate that the largest energy shift ($\sim$150 meV) of the Ir surface state towards lower binding energies is due to proximity to graphene. In other words, we suggest that the observed change of the surface state binding energy is due to a variation of the distance between graphene and the Ir surface, which in our experiments is caused either by arrays of clusters or by fabrication of several graphene layers.

In order to gain quantitative insight into this phenomenon, we have performed a DFT study of the Ir(111) surface state behaviour with variation of the graphene–Ir distance. Figure 6(c) reports the band structure of the surface state calculated for two distances providing a binding energy difference of 95 meV (energy shift similar to the shifts observed in the experiments upon deposition of large clusters (0.15 ML)). It is seen that such a shift can be achieved if the separation between graphene and Ir increases just slightly by $\sim$0.3 Å. Previously [22], it was shown that clusters decorating the moiré pattern of graphene/Ir(111) locally pin graphene to its substrate and correspondingly reduce the distance between graphene and Ir at the adsorption sites of each cluster by $\sim$1.5 Å. Such 'nail-like' spots exhibit a partial $sp^2 \rightarrow sp^3$ rehybridization of graphene [22] and act as defects that locally scatter the Ir surface state. This is consistent with the significant broadening of the surface state bands seen in figures 2 and 3. On the other hand, due to the low concentration of adsorbed cluster material the total area occupied by the clusters amounts to less than 10% of the sample surface. Considering that the pinning must induce a significant strain in the graphene, we suggest that such strain gets relieved within the graphene surface between cluster sites. As a result of such relaxation, the amplitude of the graphene corrugation is enlarged and the average distance between Ir(111) substrate and cluster-free graphene increases by $\sim$0.3 Å. Since the cluster-free area of the sample amounts to more than 90% of the total surface, the Ir surface state binding energy will on average increase and this effect will be clearly seen in ARPES dispersions. Our proposed mechanism of the structural relaxation is sketched in figure 6(d). The diagram in figure 6(e) shows the calculated dependence of the Ir surface state binding energy on the distance to graphene. The plot also comprises the variation of the relative graphene–Ir distance (Δd) in the ARPES experiment as an inset. The values of Δd were extracted by comparing the relative shifts of the Ir surface state in the experiment to the theoretical calculations in figure 6(e). It is worthwhile noting that, in the general case, such an energy shift of the surface state can be used as a probe for relaxation amplitudes in graphene. In this context, we also note that our calculations reveal that the Ir 4f core levels do not demonstrate any experimentally detectable energy shifts when the graphene–Ir separation decreases or increases (for example, for interfacial distances changing from $d = 3.3$ to 3.8 Å our calculations predict an energy shift of less than 8 meV).

Let us now briefly address the robustness of the spin structure of the Ir(111) surface state against external perturbation from the clusters. The stability of the Kramers crossing point in the case of Fe clusters (figure 3) can be explained by the absent magnetization of clusters. On the one hand, ordering temperatures of magnetic moments of individual supported clusters consisting of only a few tens of atoms (like our clusters) are below ∼10 K [39, 40], a value that is much lower than the temperature achieved in our ARPES experiments (40 K). On the other hand, even above such temperatures, disordered cluster magnetic moments may locally play a role. However, the graphene prevents direct contact between the Ir surface and the cluster magnetic moments, a fact that further supports the persistence of the Kramers degeneracy of the Ir surface state under graphene. At the same time, graphene promotes the self-assembly of deposited magnetic materials into clusters and in addition allows one to produce a gradual shift of the surface state binding energy through variable cluster superpotentials.

As seen in figure 4, graphene also protects the magnitude of the surface state Rashba splitting when high spin–orbit materials Au and Ir are deposited on the graphene moiré. The clusters are kept by the graphene overlayer relatively far from the Ir(111) substrate (at a distance of ∼2.1 Å [22]) so that the chemical interaction between clusters and the Ir surface becomes blocked and extension of the surface state wave function close to nuclei of the atoms in the clusters is prevented. The cluster-like growth regime of adsorbed Ir and Au also warrants the preservation of the structural asymmetry at the Ir(111) surface needed to maintain the large Rashba splitting of the surface state. Robustness of the Ir surface resonance against perturbations can also be related to its possible topological character discussed in our recent work [7].

Concerning the evolution of the Ir surface state binding energy upon formation of few-layer graphene (figure 5), we suggest that its origin is also mainly related to the alternating distance between Ir(111) and graphene. Each additional graphene layer should interact with the Ir substrate through van der Waals forces and 'press' the first graphene layer towards the Ir substrate [41, 42]. A reduced graphene–Ir distance, in turn, decreases the binding energy of the Rashba split surface state as shown by our DFT calculations (figure 6(c)). The surface state binding energy changes by ∼85 meV upon transition from single layer to bilayer graphene on Ir(111), which corresponds to a reduction of the graphene–Ir separation by about 0.15 Å (see the inset in figure 6(e)). At the same time the energy shift of the Ir surface state in the opposite direction upon formation of the third graphene layer can hardly be understood only in terms of the graphene–Ir separation. Indeed, the energy shift towards higher binding energies suggests that the distance between Ir and the graphene trilayer increases, which was shown not to be the case in the general situation [42]. Hence the explanation requires an additional mechanism. In this context, we would like to recall a recent publication [43] that reports different work functions for single-layer and bilayer graphene on Pd(111) and attributes this effect to the concurrence of electrostatic dipoles evolving at the graphene–Pd and graphene–graphene interfaces. We propose that the alternation of the Ir(111) surface state binding energy shift observed in our work upon formation of three graphene layers can be related to the explicit action of such interfacial dipoles, since the dipoles at the graphene–Ir and graphene–graphene interfaces must have different sign [43]. This effect competes with the decreasing distance between graphene layers and Ir(111) and apparently dominates after formation of the graphene trilayer. In figure 5(f) we observe, indeed, non-monotonic behaviour of the surface state binding energy with increasing thickness of the graphene overlayer.

5. Summary

In summary, we have reported the effect underlying two approaches that lead to a binding energy shift in opposite directions of the Rashba-split surface state of the Ir(111) surface covered with epitaxial graphene. The first approach is based on nanopatterning of the graphene moiré by periodic arrays of self-assembled nanoclusters of noble and magnetic materials. We have observed a gradual increase by up to ∼100 meV in the binding energy of the surface state with increasing cluster concentration. We have shown that neither the Kramers crossing point of spin subbands nor the magnitude of the Rashba splitting of the Ir surface state are affected by the strength of the cluster superpotential, the cluster magnetic moments or the atomic number. By means of DFT calculations, we have examined the robustness of the surface state against graphene and clusters deposited on top. Our DFT calculations reveal that the Ir(111) state is a deep surface resonance largely localized below the Ir surface. The second approach involves formation of few-layer graphene on top of Ir(111), which is achieved by segregation of carbon from the Ir bulk. In this case we have shown that, on average, the surface state shifts towards lower binding energy while preserving its spin–orbit splitting, and that for each additional graphene layer the general binding energy dependence is non-monotonic. After synthesis of three graphene layers, the surface state binding energy has decreased by ∼190 meV from the original value characteristic of bare Ir(111), while for the graphene bilayer the Ir surface state is closest to the Fermi level.

We have assigned the general dependence of the surface state binding energy to the variation of the distance between graphene and Ir(111), which results in a structural relaxation of the graphene layer. In the case of clusters, the lateral strain induced by cluster arrays leads to an enhancement of the graphene corrugation, enlargement of average graphene–Ir separation and an increase of the surface state binding energy. In the case of few-layer graphene, the formation of the additional graphene layers culminates in a decrease of the distance between Ir(111) and the first graphene layer, indicating that all new adlayers interact with the Ir substrate through van der Waals forces. Strong sensitivity of the surface state binding energy on the graphene–Ir(111) distance is confirmed by our DFT calculations.

Acknowledgments

We gratefully acknowledge computing time from the Jülich supercomputing centre (JSC). This work was supported by SPP1459 of the Deutsche Forschungsgemeinschaft and the ‘Impuls- und Vernetzungsfonds der Helmholtz-Gemeinschaft’.

References

[1] Rashba E I 1960 *Fiz. Tverd. Tela* **2** 1224
Rashba E I 1960 *Sov. Phys.—Solid State* **2** 1109
Bychkov Y A and Rashba E I 1984 *J. Phys. C: Solid State Phys.* **17** 6039
[2] Petersen L and Hedegård P 2000 *Surf. Sci.* **459** 49
[3] Bihlmayer G, Koroteev Yu M, Echenique P M, Chulkov E V and Blügel S 2006 *Surf. Sci.* **600** 3888
[4] Nagano M, Kodama A, Shishidou T and Oguchi T 2009 *J. Phys.: Condens. Matter* **21** 064239
[5] Rotenberg E, Chung J W and Kevan S D 1999 *Phys. Rev. Lett.* **82** 4066

[6] Shikin A M, Varykhalov A, Prudnikova G V, Usachov D, Adamchuk V K, Yamada Y, Riley J D and Rader O 2008 *Phys. Rev. Lett.* **100** 057601
[7] Varykhalov A, Marchenko D, Scholz M R, Rienks E D L, Kim T K, Bihlmayer G, Sánchez-Barriga J and Rader O 2012 *Phys. Rev. Lett.* **108** 066804
[8] Varykhalov A, Sánchez-Barriga J, Shikin A M, Gudat W, Eberhardt W and Rader O 2008 *Phys. Rev. Lett.* **101** 256601
[9] Crepaldi A *et al* 2012 *Phys. Rev. Lett.* **109** 096803
[10] Murakami S, Nagaosa N and Zhang S-C 2003 *Science* **301** 1348
[11] Sinova J, Culcer D, Niu Q, Sinitsyn N A, Jungwirth T and MacDonald A H 2004 *Phys. Rev. Lett.* **92** 126603
[12] Hochstrasser M, Tobin J G, Rotenberg E and Kevan S D 2002 *Phys. Rev. Lett.* **89** 216802
[13] Barke I, Zheng F, Rügheimer T K and Himpsel F J 2006 *Phys. Rev. Lett.* **97** 226405
[14] Ast C R, Henk J, Ernst A, Moreschini L, Falub M C, Pacilé D, Bruno P, Kern K and Grioni M 2007 *Phys. Rev. Lett.* **98** 186807
[15] N'Diaye A T, Coraux J, Plasa T N, Busse C and Michely Th 2008 *New J. Phys.* **10** 043033
[16] Coraux J, N'Diaye A T, Engler M, Busse C, Wall D, Buckanie N, Meyer zu, Heringdorf F-J, van Gastel R, Poelsema B and Michely Th 2009 *New J. Phys.* **11** 023006
[17] Starodub E, Bostwick A, Moreschini L, Nie S, El Gabaly F, McCarty K F and Rotenberg E 2011 *Phys. Rev.* B **83** 125428
[18] Pletikosić I, Kralj M, Pervan P, Brako R, Coraux J, N'Diaye A T, Busse C and Michely Th 2009 *Phys. Rev. Lett.* **102** 056808
[19] N'Diaye A T, Gerber T, Busse C, Myslivecek J, Coraux J and Michely T 2009 *New J. Phys.* **11** 103045
[20] Rusponi S, Papagno M, Moras P, Vlaic S, Etzkorn M, Sheverdyaeva P M, Pacilé D, Brune H and Carbone C 2010 *Phys. Rev. Lett.* **105** 246803
[21] Sánchez-Barriga J, Varykhalov A, Marchenko D, Scholz M R and Rader O 2012 *Phys. Rev.* B **85** 201413
[22] Feibelman P J 2008 *Phys. Rev.* B **77** 165419
[23] Varykhalov A, Rader O and Gudat W 2005 *Phys. Rev.* B **72** 115440
[24] Nie S, Walter A L, Bartelt N C, Starodub E, Bostwick E, Rotenberg A and McCarty K F 2011 *ACS Nano* **5** 2298
[25] Vlassiouk I, Regmi M, Fulvio P, Dai S, Datskos P, Eres G and Smirnov S 2011 *ACS Nano* **5** 6069
[26] Hattab H *et al* 2011 *Appl. Phys. Lett.* **98** 141903
[27] Marchenko D, Sánchez-Barriga J, Scholz M R, Rader O and Varykhalov A 2013 *Phys. Rev.* B **87** 115426
[28] Wimmer E, Krakauer H, Weinert M and Freeman A J 1982 *Phys. Rev.* B **24** 864
[29] Wortmann D, Ishida H and Blügel S 2002 *Phys. Rev.* B **66** 075113
[30] Krupin O, Bihlmayer G, Starke K, Gorovikov S, Prieto J E, Döbrich K, Blügel S and Kaindl G 2005 *Phys. Rev.* B **71** 201403
[31] Potter A C and Lee P A 2011 *Phys. Rev.* B **83** 184520
[32] Rader O, Varykhalov A, Sánchez-Barriga J, Marchenko D, Rybkin A and Shikin A M 2009 *Phys. Rev. Lett.* **102** 057602
[33] Varykhalov A and Rader O 2009 *Phys. Rev.* B **80** 035437
[34] Varykhalov A, Sánchez-Barriga J, Shikin A M, Biswas C, Vescovo E, Rybkin A, Marchenko D and Rader O 2008 *Phys. Rev. Lett.* **101** 157601
[35] Marchenko D, Varykhalov A, Scholz M R, Bihlmayer G, Rashba E I, Rybkin A, Shikin A M and Rader O 2012 *Nature Commun.* **3** 1232
[36] Varykhalov A, Scholz M R, Kim T and Rader O 2010 *Phys. Rev.* B **82** 121101
[37] Varykhalov A, Marchenko D, Sánchez-Barriga J, Scholz M R, Verberck B, Trauzettel B, Wehling T O, Carbone C and Rader O 2012 *Phys. Rev.* X **2** 041017
[38] Vinogradov N A *et al* 2012 *Phys. Rev. Lett.* **109** 026101
[39] Gambardella P *et al* 2003 *Science* **300** 1130

[40] Dürr H A, Dhesi S S, Dudzik E, Knabben D, van der Laan G, Goedkoop J B and Hillebrecht F U 1999 *Phys. Rev.* B **59** R701 and references therein
[41] Adamska L, Lin Y, Ross A J, Batzill M and Oleynik I I 2012 *Phys. Rev.* B **85** 195443
[42] Zheng J, Wang Y, Wang L, Quhe R, Ni Z, Mei W-N, Gao Z, Yu D, Shi J and Lu J 2013 *Sci. Rep.* **3** 2081
[43] Murata Y, Nie S, Ebnonnasir A, Starodub E, Kappes B B, McCarty K F, Ciobanu C V and Kodambaka S 2012 *Phys. Rev.* B **85** 205443